

PROCEEDINGS SERIES

PLASMA PHYSICS
AND CONTROLLED
NUCLEAR FUSION RESEARCH
1974

PROCEEDINGS OF THE
FIFTH INTERNATIONAL CONFERENCE ON PLASMA PHYSICS
AND CONTROLLED NUCLEAR FUSION RESEARCH
HELD BY THE
INTERNATIONAL ATOMIC ENERGY AGENCY
IN TOKYO, 11-15 NOVEMBER 1974

In three volumes

VOL. III

INTERNATIONAL ATOMIC ENERGY AGENCY
VIENNA, 1975

MAJOR DESIGN FEATURES OF THE CONCEPTUAL D-T TOKAMAK POWER REACTOR, UWMAK-II

R. W. CONN, G. L. KULCINSKI, M. A. ABDOU,
R. W. BOOM, G. A. EMMERT, J. KESNER,
C. W. MAYNARD, A. T. MENSE, J. E. SCHARER,
T. SUNG, I. SVIATOSLAVSKY, D. SZE,
W. VOGELSANG, L. WITTENBERG, T. YANG,
W. YOUNG

Fusion Technology Program,
University of Wisconsin,
Madison, Wis.,
United States of America

Abstract

MAJOR DESIGN FEATURES OF THE CONCEPTUAL D-T TOKAMAK POWER REACTOR, UWMAK-II.

The conceptual design of a 5000 MW(th) (~1700 MW(e)) helium-cooled tokamak fusion reactor is presented. The fuel is deuterium and tritium and the structural material is 316 stainless steel. The design has a low aspect ratio (2.6) and low toroidal field on axis (35.7 kG) with 24 extended "D"-shaped superconducting TF coils. A superconducting air core transformer is designed with windings outside TF coils while the vertical field magnets, also superconducting, are inside the extended "D's". The plasma operating conditions have been determined using pessimistic scaling laws resulting from the trapped-ion instability. Such scaling can be beneficial in the reactor regime. A double-null poloidal field divertor is included for impurity control and a two-dimensional woven carbon cloth mounted on the vacuum chamber wall is included to protect the plasma from high-Z impurities and the first structural wall from erosion by charged-particle bombardment. The helium-cooled blanket contains solid Be in canned rods for neutron multiplication and solid lithium aluminate, also in canned rods, for tritium breeding. The breeding ratio is 1.19, the energy per fusion is 21.56 MeV, and the tritium inventory in the blanket is low, 42 g. Radiation damage problems are similar and as serious as those found in our previous study. Periodic replacement of blanket modules every two years will probably be required because of radiation damage. A detailed mechanism for blanket removal that does not require removal of the shield or the VF and TF coils is presented.

I. Introduction and Overview

The conceptual design of fusion reactors has become an important area of research in fusion technology. The aim of these studies is to perform a self consistent and thorough analysis of probable future fusion power reactors in an effort to assess the technological problems posed by such systems and to examine feasible solutions. Such work helps provide a perspective on the relative difficulties and importance of various technical problems and acts as a guide for further research. In earlier work, we presented a conceptual tokamak fusion reactor design, UWMAK-I^[1-3] based on the D-T cycle with liquid lithium acting as the coolant, moderator, and tritium breeding material and 316 stainless steel as the structure. That design is conservative in terms of materials choices and operating conditions and it generated several fundamental results. One of the most important is the apparent need to periodically replace the reactor first walls because of radiation damage.

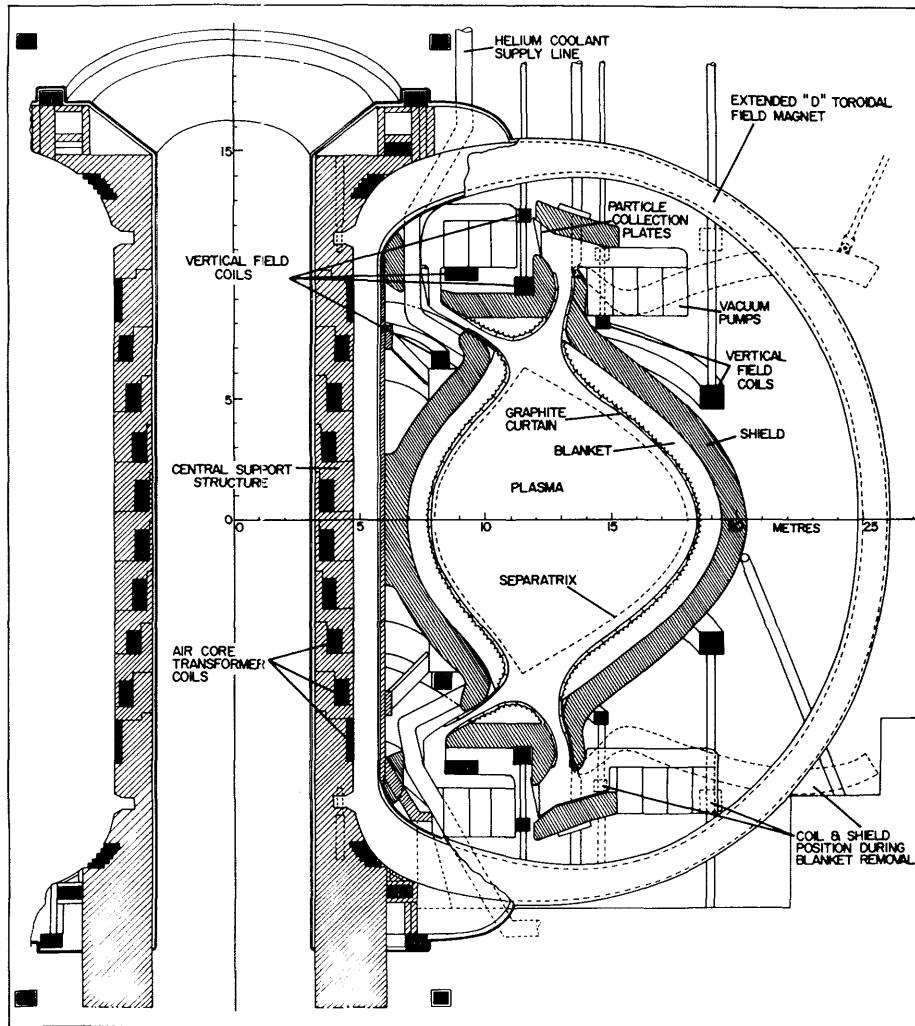


FIG. 1. Cross-section view of UWMAK-II

Overall, there are many advantages to a system like UWMAK-I and these are documented in references 1-3. Nevertheless, two of the major areas of concern were the maximum temperature limit of 500°C in the stainless steel due to compatibility problems and the relatively large tritium inventory (8.7kg) in the liquid lithium coolant. In addition, there were twelve toroidal field coils which produced a large ($\sim 20\%$) field ripple and the removal and disassembly of the first wall for repair or replacement involved moving very heavy modules (3500 metric tons).

In this paper, we discuss the conceptual design of a similarly sized reactor (5000MW(th)), UWMAK-II, which would be constructed of stainless steel and cooled with helium. A cross section view of the UWMAK-II system is shown in

TABLE I. BURN CYCLE FOR UWMAK-II

Current Rise Time	Heating for Ignition & to Thermally Stable Operating Point	Burn Time	Plasma Current Turn Off	Purge Chamber	Reset Transformer Coils	Total Cycle
10 s	20 s	5400 s	100 s	50 s	150 s	5730 s

Figure 1. UWMAK-II is a low aspect ratio, low field design, as in UWMAK-I, and includes a double null, axisymmetric poloidal field divertor for impurity control. In addition, a carbon curtain, made of two dimensional woven carbon fiber is mounted on the first vacuum chamber wall to protect the plasma from high Z impurities and to protect the first wall from erosion by charged particle bombardment. (This concept is relevant to present experiments as well as reactors.⁽⁴⁾) The maximum pressure of the helium coolant in the blanket is

750 psia and the blanket contains beryllium for neutron multiplication and solid lithium aluminate (LiAlO_2) as the breeding material. The lithium is enriched to 90% ^6Li and gives a breeding ratio of 1.19. The total energy per fusion is 21.6 MeV, which is fairly high. In addition, the use of solid breeding material has made the tritium inventory in the blanket very low, approximately 42 g. The radiation damage problems are similar to those in the UWMAK-I study^[1,5] and the results for UWMAK-II again indicate that periodic replacement of the first 20 cm of the blanket modules approximately every two years will be required.

The toroidal field (TF) magnets are a set of 24 "extended D" superconducting coils of NbTi in Cu with stainless steel structure. The extension of the "D" shape beyond the outside edge of the shield allows the shield to be opened as indicated in Fig. 1 and a blanket removed between coils without removing the TF coils. The vertical field (VF) coils have been placed inside the TF coils to minimize the energy stored in the poloidal magnetic field. This value is now 10.4×10^9 joules compared to 53.4×10^9 joules in UWMAK-I where the VF windings were placed outside the TF coils. The design philosophy for the coils is crucial when they are placed inside the TF set and this is discussed in section III. A superconducting air-core transformer is used and the transformer (OH) windings are outside the main TF coils.

In the next three sections, we discuss the main technical aspects of the UWMAK-II study together with the analysis and resolution of many of the technical problems such a system would pose.

II. Plasma Aspects of UWMAK-II

We discuss in this section the problems of energy storage and plasma current rise time, heating to ignition, plasma operating conditions, divertor operation and particle collection, and anticipated impurity levels. We will also briefly describe the use of a carbon "curtain" mounted on the vacuum chamber wall to protect the plasma from high Z impurities and protect the first wall from surface erosion by charged particles.

The plasma current is assumed to rise linearly to its final value of 14.9 MA in 10 seconds. The method for carrying this out can be based on an expanding limiter concept, such as will be employed on PLT,^[6] or an expanding magnetic limiter, such as is proposed for the poloidal divertor experiment, PDX^[7]. An air core transformer has been designed with superconducting coils outside the toroidal field magnets at positions shown in Figure 1. The coils follow a flux surface as closely as possible and the maximum field leakage in the vacuum chamber is about 100 G.

A postulated burn cycle for UWMAK-II is given in Table I. The long burn time is assumed on the basis of a model calculation for divertor performance and the use of a carbon curtain to eliminate the source of high Z impurities

during the burn. Both points are discussed shortly. During the 10 sec current rise time, the transformer is discharging while the VF coils shown in Fig. 1 must rise with the plasma current. The power to drive the VF windings comes from the line and from an energy storage unit. Assuming 500 MW can be purchased from the line, an energy storage system must provide 0.26 MW-hr in 3.75 sec, a quite reasonable energy transfer, with an associated maximum power of 500 MW. The energy storage unit uses an improved discharge circuit^[8] much like a 3 phase, ac/dc Graetz bridge and the bridge costs are about \$15/kWe. We have used \$20/kWe for bridges to transfer power from the line. The capital costs for a nominal 1 MW-hr storage unit^[9] is about \$15 x 10⁶ giving a total cost for the storage unit and delivery system of about \$32.5 x 10⁶.

The maximum energy stored in the poloidal field is 2.9 MW-hr and occurs at the end of the burn. This energy is given back to the line in approximately 100 sec. Following a 50 sec purge of the vacuum chamber, the transformer is then reset in an additional 150 sec. The bridges provided to transfer power during startup are more than sufficient to handle transfers at the end of the burn.

AC losses in the normal conductors have been analyzed and found to be about 5.2 kW-hr per charge at 4.2°K. This corresponds to about 1.6 MW-hr in refrigeration losses. However, this energy need not be supplied over 10 sec but can be supplied by liquifying helium during the burn time. The extra refrigeration power is a nominal 1 MW and the additional helium required is about 7000 liters, or about 10% of the helium used to fill the dewars of the OH and VF coils. The maximum eddy current loss in the coils is at the point of maximum field and amounts to about 0.14 w/cm² in the largest VF coil, a very small value compared to the I²R losses if the magnet goes normal. Thus, the copper temperature will remain about 4.2°K during the 10 second plasma current rise phase.

During the current rise, the plasma is heated only by ohmic heating and reaches a temperature of approximately 1.5 keV. Supplemental heating is thus required to achieve ignition and we have studied the use of high energy neutral beams for this purpose. In earlier work^[1,10], we examined this question assuming the plasma electrons followed pseudoclassical scaling^[11,12] while the ions followed neoclassical theory.^[13] In this work, we have made the pessimistic assumption that trapped particle instabilities^[14,15] will govern the plasma transport in less collisional regimes than present experiments achieve. The diffusion coefficients have been estimated for the trapped electron^[11] and trapped ion^[12] instabilities from a quasi-linear type of analysis^[18] by using

$D_{\perp} = \frac{\gamma}{k_{\perp}^2}$, where γ is the linear growth rate. Of course, in the low collision frequency regime, only theoretical estimates are available for such scaling formulae and these are relatively crude.^[15] In practice, the modes may saturate at lower levels and/or be more localized in space. Thus, we have tried to examine a worst case and the results should be viewed in that light. We have also included in the plasma energy balance equations the radiative losses from line and recombination radiation.^[19]

Time dependent, space independent plasma particle and energy balance equations have been used to study the heat up phase and to determine conditions characterizing the plasma during the burn phase. The results from the space independent model are found to give good agreement (within about 10%) for average densities and temperatures with more detailed space-time calculations.^[10]

One effect of the pessimistic microinstability scaling laws is that it is not possible to achieve ignition at relatively low average densities, such as $n_e \sim 1.5 \times 10^{13} \text{ cm}^{-3}$ used previously.^[1,10] The reason is the alpha power varies as n_1^2 whereas D_{\perp} for the trapped ion mode,^[15] which governs as ignition conditions are approached, varies inversely with n_1 . The minimum average electron density for which we obtain ignition is found to be approximately $4 \times 10^{13} \text{ cm}^{-3}$. This is relevant since it implies neutral beams will not effectively penetrate

TABLE II. PLASMA OPERATING PARAMETERS FOR UWMAK-II

Plasma Radius	5m	Average Ion Temperature	15.2 keV
Major Radius	13m	Average Electron Temperature	13.5 keV
Aspect Ratio	2.6	Confinement Time	4 sec
First Wall Radius	5.5m	Average Ion Density	$6.46 \times 10^{13} \text{cm}^{-3}$
Chamber Wall Area (actual)	3300m^2	Average Alpha Density	$0.09 \times 10^{13} \text{cm}^{-3}$
Plasma Current	14.9MA	Average Electron Density	$6.64 \times 10^{13} \text{cm}^{-3}$
Poloidal Beta	2.3	Fractional Burnup	2.75%
Stability Factor, q(a)	2.3	Power to Divertor	716 MW
Toroidal Field (on axis)	35.7kG	(in Particles)	
Anomalous Resistivity		Radiation Wall Loading (Max.)	3.42 w/cm^2
Factor	3	Neutron Wall Loading (Max.)	1.16 MW/m^2

such plasmas unless the beam energy exceeds about 700 keV. In contrast, a low density startup, as can be achieved with more favorable scaling laws,^[11,12] does not require energies that high.^[10]

At $n_e \sim 4 \times 10^{13} \text{cm}^{-3}$, it is found that 60 MW of injected power can ignite the plasma in 10 seconds. If the beams are turned off just after ignition, the time to the plasma operating conditions is approximately 80 seconds. However, the beams can be left on after ignition so as to reach the thermally stable operating conditions approximately 10 seconds after ignition. Thus, for UWMAK-II, the overall time from startup to the operating point is taken as 30 seconds.

For impurity control, we have analyzed the operation of a double null poloidal divertor generated by the coils shown in Figure 1. These coils simultaneously provide the vertical field required for equilibrium of the plasma column. The separatrix and two neutral points are also indicated on Figure 1. The general features of the divertor are much the same as in the UWMAK-I divertor design^[11] except that the divertor coils are now inside the toroidal "D" coils. This reduces the stored magnetic energy but presents a construction and maintenance problem. Since it will not be practical to replace a malfunctioning coil, the coils must be designed for high reliability. The coil design philosophy is discussed in detail in section III.

The effectiveness of the divertor in reducing the charged particle flux to the wall has been estimated using a simple model where the plasma density profile in the scrape-off region is determined by cross-field diffusion (with some coefficient D_{\perp}) and by plasma flow along the diverted field lines to the particle collectors on a time scale $\tau_{||}$. The characteristic scale length, d , for the density profile is $\sqrt{D_{\perp} \tau_{||}}$. Larger values of d are better for ionization of entering impurities before they get to the separatrix while small d is better for reducing wall erosion. A pessimistic choice of D_{\perp} is $\sim 0.1 D_{\text{Bohm}}$. One may visualize the Bohm-like scaling to come from low frequency turbulence caused by steep density gradients in the scrape-off zone. A minimum value for $\tau_{||}$ is L/v_S where L is the distance along the field lines to the collectors and v_S is the ion sound speed ($v_S = [\text{Max}(T_i T_e)/m_i]^{1/2}$). In the outer divertor (Fig. 1), the plasma must pass through a region of higher B on its way to the collector so that magnetic mirroring can be important in determining $\tau_{||}$. The plasma, however, would have a loss-cone distribution and thus be susceptible to all the usual microinstabilities associated with mirror machines.^[20] These instabilities will have the effect of filling the loss-cone on a time scale comparable to L/v_S . Thus, we have chosen $\tau = L/v_S$ in our model. This model gives a characteristic thickness $d \sim 2-3$ cm which is quite small compared with the 50 cm wide scrape-off zone. As a consequence, the divertor is very effective at preventing charged particles from reaching the wall but ineffective at ionizing impurities before they reach the separatrix.

Since neutron sputtering will generate impurities that can return to the plasma, we have developed the concept of using a 2 dimensional woven carbon cloth as a curtain to protect the vacuum chamber wall. Detailed analysis of the carbon curtain performance is presented elsewhere. The results show that much higher levels of carbon (up to several percent) can be tolerated compared with high Z impurities such as Fe, Mo, and W. Further, we have estimated impurity levels using a simple model such as that discussed by Duchs et al.^[21] Assuming the divertor is greater than 99% efficient at collecting particles diffusing from the plasma but only 10% efficient at shielding the plasma the carbon concentration ($\frac{n_c}{n_e}$) is calculated to be 0.02% assuming the impurity confinement time, τ_{imp} , is equal to $\tau_{D,T}$. For $\tau_{imp} = M \tau_{D,T}$, one finds $\frac{n_c}{n_e} = .0002M$. Thus, M multiples of 100 to 1000 may be acceptable under these circumstances and allow long burn times.

Based on this analysis, it is assumed that the levels of low Z impurities in the plasma are essentially negligible and that there are no sources of high Z impurities. The plasma operating conditions have then been calculated using energy balance equations including alpha heating, radiation losses, and energy losses based on estimated trapped particle mode scaling laws. The plasma conditions characterizing UWMAK-II during the burn phase are given in Table II. We have imposed the values of stability factor and poloidal beta as indicated and β_0^e is about 1. Note that the particle leakage rate is high reflecting the impact of trapped ion mode scaling. Interestingly, however, this scaling is adequate and leads to thermally stable operating conditions in the optimum 10-20 keV range. With a confinement time of 4 sec, it is assumed that fueling, perhaps with pellets^[22], maintains the desired plasma density.

The high particle leakage rate coupled with an efficient divertor for collecting particles diffusing from the plasma means 716 MW(th) is associated with this particle diffusion. This presents an average thermal load on the collector system of about 3 MW/m². The peak power may be as high as 10-20 MW/m² and presents a formidable problem. In our previous work^[1-3], liquid lithium flowing along a plate was used but this will not now be adequate. Thus, it is proposed that this large particle flux be collected by two lithium streams, a primary free falling lithium film and a backup lithium film flowing on a stainless steel plate. These are shown in Fig. 1. The free falling stream can attain adequate velocities (~6 m/sec) to keep the maximum temperature to about 350°C. The main difficulty is that this stream may not be stable and, because of the high surface tension of lithium, may break into columns. The high surface tension will, however, keep the film from spraying when collected and the backup film should collect any particles passing through the primary lithium sheet.

III. Magnets for UWMAK-II

There are 24 modified constant tension "D" shaped toroidal field magnets which produce the required on-axis field of 35.7 kG. The maximum field at the innermost portion of the magnet (at R = 5.75m) is 83 kG. The energy stored in the toroidal field is 61.9 MW-hr or 223 GJ. The conductor is NbTi superconductor embedded in a copper stabilizer. The basic conductor design and stress analysis follows our earlier work.^[1] The maximum conductor cross section is 2.87 cm (width) by 1.90 cm (thickness) and tapers linearly in both width and thickness to 1.70 cm by 1.13 cm at the outside turn. Each magnet is composed of 19 forged discs with 58 conductor turns per disc. The conductor current is 9065 A with 19 discs, 10,131 A with 17 discs, and 11,481 A with 15 discs connected. Thus, a current margin of 27% over normal operation is included. In addition, the normal operating current with 19 discs is 13.3% lower than capability. Extra discs and extra current capabilities have been included to enhance reliability and allow the design assumption that planned periodic removal of the TF coils over a plant lifetime is not required.

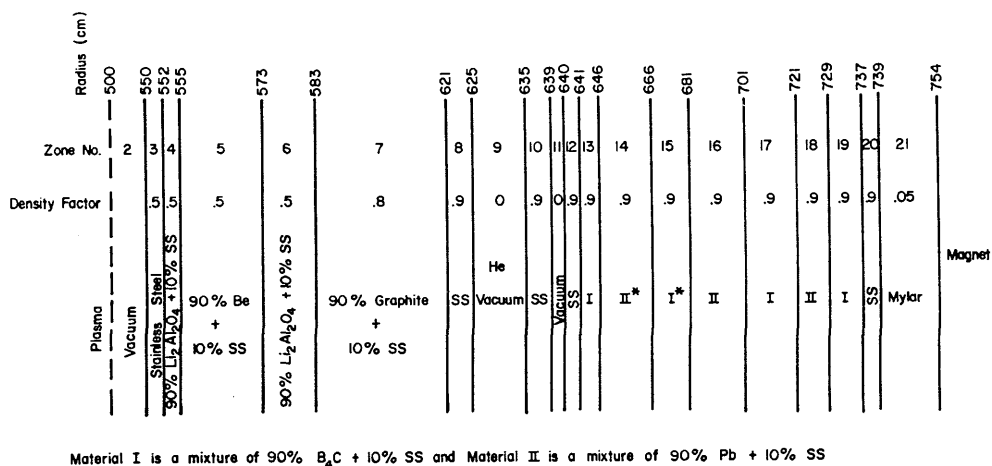


FIG. 2. A schematic of UWMAK-II blanket and shield.

The extension of the TF coil beyond the outer edge of the shield (see Fig. 1) is included to allow removal of the blanket modules between TF coils without requiring any of the coils themselves to be removed.

To provide this circumferential clearance, it is necessary to extend the outer portion of the "D" coils to a larger major radius. This in turn would create a very tall and costly magnet if the constant tension design were adhered to. In order to use a modified "D", no higher than is required to accommodate the system components which are placed inside the TF coils, it is necessary to deviate from a constant tension design and provide for bending in the discs and for support from the central core over a portion of each toroidal field magnet.

The design presented is a constant tension design with no bending stresses present in the outer half section of the coil. Inside a major radius of about 13 m, the forged discs are increased in thickness in order to sustain the bending stresses and hoop stresses created by the magnetic loading. In this region, the conductor size and spacing is maintained as elsewhere but kept to the inside edge of the disc. This minimizes the stresses and the stored magnetic energy.

Calculations reveal that the increased dimensions of the forged discs, shown in Figure 1, are not sufficient to keep the stresses and deflections to acceptable levels. The central cylindrical support core has therefore been extended in the regions directly above and below each toroidal field magnet to provide additional support. This cantilever support is sized in conjunction with the increased magnet dimensions in this region in order to keep the maximum stress in the stainless steel discs to less than $4.14 \times 10^8 \text{ N/m}^2$ (60 Kpsi) and to match the slope and deflection at the end of the reinforced portion of the magnet to those of the constant tension outer part.

At the design maximum stress level in the stainless steel discs, the copper will yield but the maximum strain will not exceed 0.2% and the resistivity of the copper will not be degraded significantly.

The OH and VF coils are designed for standard jelly-roll construction using a copper and NbTi composite developed at NAL.^[23] An individual conductor carries 20,000 A and the overall design current density is a conservative 1500 A/cm^2 .

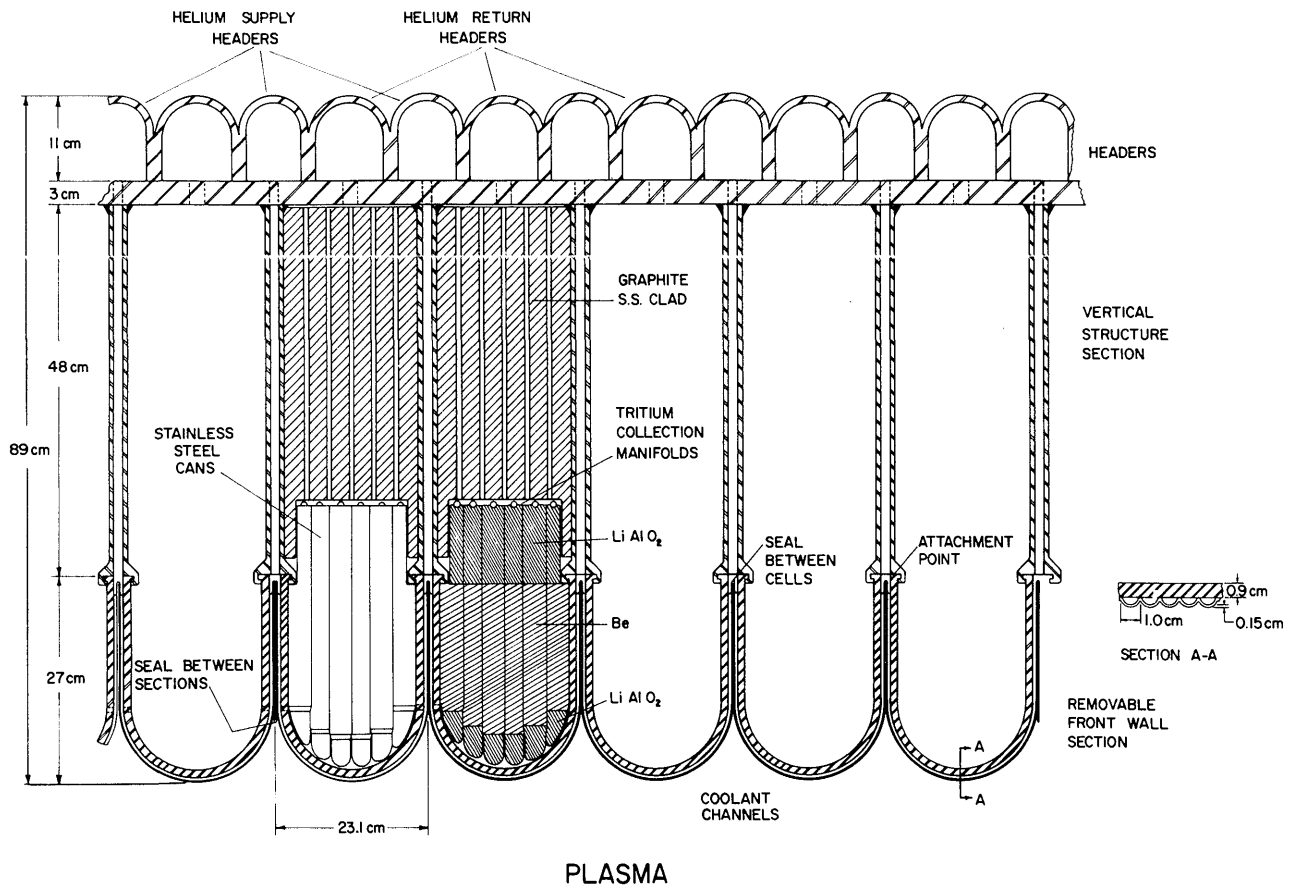


FIG. 3. Blanket section for UWMK-II.

TABLE III. PROPERTIES OF UWMAK-II BLANKET AND SHIELD

Thermal Power	5000 MW(th)	Li Inventory in Blanket	8×10^4 kg
Electric Power	1700 MW(e)	T ₂ Inventory in Blanket	42.0 g
Power (Blanket)	4232 MW(th)	T ₂ Leakage Rate	2.0 Ci/d
Power (Shield)	52 MW(th)	Coolant	Helium
Structural Material	316 SS	Max. Pressure Drop	32 psi
Max. dpa rate in 1st Wall	17 yr ⁻¹	He Flow Rate	4300 kg/sec
Max. He Prod. Rate in 1st wall	292 appm y ⁻¹	Coolant Pumping Power	300 MW(e)
Max. Wall Erosion Rate	0.15 mm y ⁻¹	Coolant Inlet Temp.	~450°C
Anticipated First Wall Life	2 years	Coolant Outlet Temp.	650°C
First Wall Temp. (max)	550°C	Breeding Ratio	1.19
Max. Structure Temp.	654°C	Energy Per Fusion	21.56
Carbon Curtain Temp.	900°C	Energy Attenuation to Magnets	6×10^{-8}
Max. dpa Rate in Curtain	5 y ⁻¹		

The turns are wound with four conductors in parallel and these parallel conductors are transposed during winding to equalize the separate inductances and currents. The design stress levels are the same as for the TF coils and the cooling conditions are the standard nucleate boiling limits of 0.1 to 0.4 w/cm², depending on surface location. Liquid helium pool cooling at 4.2 K is used throughout.

As with the TF coils, the OH and VF windings shown in Fig. 1 are designed with redundancy such that the possibility of major coil failure is minimized. For example, the failure of some conductors can be compensated by increased current density in the remaining conductors. The redundancy includes 10% extra turns and 10% extra allowance in detail design. The coils could thus operate with 20% of the turns disconnected. A major difficulty is the winding of these coils in place. An internal winding machine on tracks running around the major circumference inside the 24 modified "D" TF magnets is envisioned. The extension of the TF coil, although for other reasons, provides added space for such an operation. Coil removal would require either unwinding or cutting through but it is felt that the low current density and redundant design will make coil replacement unlikely over the plant lifetime.

Extending the TF coils in the low field region and including non-constant tension portions has increased the overall cost of the TF coil set relative to UWMAK-I.^[1] However, the energy stored in the poloidal field is only 2.9 MW-hr so that the OH and VF sets are much less expensive than in the previous design. A more detailed cost analysis for the magnets, refrigerators, power supplies, and energy storage unit yields a total estimated cost of $\$285 \times 10^6$. Our earlier UWMAK-I magnet system has been re-analyzed in greater detail and found to cost approximately the same. However, the many additional design advantages, such as individual removal of blanket modules, better VF control, and a relatively short 10 sec current rise time, tend to favor the UWMAK-II approach.

IV. Blanket and Shield Considerations for UWMAK-II

The design of the blanket and shield for UWMAK-II is based on two essential criteria: 1) to achieve high tritium concentrations to ease tritium recovery; and 2) to achieve a low tritium inventory. These design criteria preclude the use of liquid lithium as the coolant. Under these circumstances, the natural coolant choice is He which avoids the compatibility and pressure limitations of water and the temperature and compatibility problems of molten salts. For the structural material, we have chosen 316 stainless steel for reasons outlined previously.^[1,2] In addition,

excessive oxidation by small oxygen concentrations in He ruled against niobium and vanadium while the aluminum alloys are subject to combined high helium production rates and low temperature stress limits.

Pumping difficulties in small liquid lithium zones make the use of a solid breeder material, as in recent breeding concepts of Powell et al. [24], very attractive. A review of the properties of various alloys and compounds of lithium led to the choice of LiAlO_2 as the breeding material because of its high melting point and apparently acceptable tritium diffusion properties.

The requirement of a small lithium inventory results in the need for a large tritium production cross section to reduce the neutron mean free path significantly. This can be achieved by enriching the lithium to 90% ^6Li and then using slow neutrons in the breeding process. A concomitant is the need for a neutron multiplying material to insure adequate tritium production. The material choice is beryllium or one of its compounds. A potential resource problem for beryllium makes it desirable to minimize its use subject to the breeding constraint. Tritium and energy production calculations indicate metallic beryllium is the most suitable choice here. In addition, neutron conservation considerations have resulted in the choice of graphite as a neutron reflecting material.

These many considerations have led to the detailed blanket and shield design shown in Figs. 2 and 3. Fig. 2 is a schematic used for neutronics and photonics calculations while Fig. 3 shows the actual blanket cross section.

The first structural (or vacuum) wall of stainless steel is about 2 cm thick and contains He flow channels. Thus neutronic calculations were made with a 50% density factor. The blanket is constructed of cells containing the lithium aluminate and beryllium in stainless steel clad pins having a 3.75 cm diameter, a 31 cm length, and a 0.05 cm wall thickness. These tubes are closed at one end and attached to a small gas plenum at the other end for tritium extraction. The 0.5 density factors are introduced to account for voids since the Be and LiAlO_2 will be microspheres of about 20 microns in radius. The graphite reflector is canned in stainless steel and cooled by the main He stream.

The shield consists of stainless steel support zones and alternating layers of B_4C and Pb, as shown in Fig. 2. Zone 11 is an insulating gap to separate the high temperature blanket from the low temperature shield. The shield design has been optimized using methods described earlier. [1,25] The major parameters characterizing the many and varied aspects of the UWMAK-II blanket and shield system are summarized in Table III.

The radiation damage in the stainless steel first wall is similar to (and as serious as) that found in the earlier UWMAK-I design [1-3,5] and the wall life is still limited to about 2 years by loss of ductility. Wall erosion is less of a problem due to the carbon curtain. Radiation damage in the shield and magnet is generally less severe than in the earlier design.

Turning to the new radiation damage problems in UWMAK-II, we first examine the carbon curtain. It is calculated that the displacement damage is ~5 dpa per year. If the curtain operates at 800-900°C (4-8 w/cm²), a few percent shrinkage per year for the first few years is expected, but this would probably be followed by expansion and the curtain may be in a "run away" swelling mode in 5 years. It thus seems prudent to change the curtain every 2 years. Another potential problem in the carbon is the high helium gas production rate of ~3100 appm/year. Such high helium contents have never been investigated for carbon and this alone would suggest a two year replacement time.

Another major problem is the very high helium and hydrogen gas generation rates in the LiAlO_2 . It is calculated that ~22,000 appm/year of helium and a similar amount of tritium will be generated per year. It is almost certain that the ceramic will not contain such high gas contents. The swelling values are uncertain at this time because the amount of

helium escaping from the powder cannot be calculated. However, the LiAlO_2 must be changed every two years in any case, due to high burn up of the lithium, so that long term operation is not required.

The Be neutron multiplier generates helium gas by four reactions which leads to a maximum of 3040 appm/year in the Be nearest the plasma. The swelling that such a large helium concentration induces is a function of the bubble size. For diameters greater than 300-400 Å, swelling of more than 30-40% per year might be expected. Such large swelling values are not tolerable and more work is needed on this topic.

In the graphite reflector, the displacement rate is 1.25 dpa/year. At this rate, the graphite will shrink somewhat in the first two years but runaway swelling may occur after 10 years depending on the degree of anisotropy in the graphite. Hence it may be necessary to change the reflector every 10-15 years.

The radioactivity of the design is dominated by the stainless steel, as in UWMAK-I,^(1,26) and is generally comparable in the two systems. The neutron spectrum is somewhat softer in the current design but there is more steel present. These are compensating effects and the result is a rather nominal increase of the radioactivity by a factor of two or less in UWMAK-II over its predecessor, depending on the time of comparison.

Unit shield costs were assumed lower in the current design (reflecting a drop in the price of B_4C) and led to a much more effective shield at optimum. The result is the activity and afterheat in the magnet is greatly reduced compared to UWMAK-I. For example, in the 10cm of magnet material immediately behind the shield, the decay heat at shutdown is only $1.4 \times 10^{-8}\%$ of the operative power which will significantly reduce access and maintenance problems in the magnets.

The helium coolant will enter the blanket modules at a pressure of 50 atm. In order to separate the regions with high stress and low strength, the coolant is directed first to the first wall and then to the blanket zones where most of the energy is generated. Note that over one-third of the heating is in the lithium bearing zones. A layer of small coolant channels is located on the plasma side of the first wall to absorb the surface heating and to reduce the thermal stress in the main wall. (See Fig. 3) The maximum first wall temperature is 550°C . The coolant then flows back across the tubes containing the LiAlO_2 , the Be and the graphite. The total pressure drop through the reactor is 32 psi and requires 300 MW(e) of pumping power. The major heat transfer parameters are listed in Table III.

The surface temperature of the stainless steel clad pins containing LiAlO_2 is found to be about 600°C . Since the thermal conductivity of LiAlO_2 is very low, the centerline temperature is over 1300°C and the average temperature is approximately 900°C . The resulting diffusion coefficient limits the tritium path to about 10 microns if the tritium inventory is to be kept below 100 grams. This requires either a powder of $\sim 20 \mu\text{m}$ diameter particles or a porous medium with pores about $20 \mu\text{m}$ apart. If the surrounding medium is maintained at a tritium partial pressure of 10^{-4} torr, the solubility of tritium in LiAlO_2 leads to a 42.0g inventory.

The tube surface area is quite large, on the order of $3 \times 10^8 \text{cm}^2$, and tritium diffusion through the tube walls into the main helium coolant system and then to the steam system could reach approx. 13 grams/day. To prevent this tritium from reaching the environment, 10^{-2} torr of oxygen (O_2) is introduced into the coolant to react with the tritium and form T_2O . The T_2 pressure drops to 1.6×10^{-14} torr and only 2.0 Ci/day of tritium will reach the steam system.

The T_2O will be absorbed in molecular sieves to keep the T_2O vapor pressure below 10^{-3} torr. Of the 10^6 gram-moles of helium in the

cooling system, only 1.2% of the helium need transit the absorption bed on each cycle. Almost 80 grams/day of tritium diffuses into the helium resulting in 13.6 gram-moles of T_2O . Using an absorption limit of 640 kg/m³ of molecular sieves, the absorption bed requires only 0.07 m³ of molecular sieves for one day's generation of T_2O in the helium.

From a mechanical design viewpoint, the blanket of UWMAK-II consists of three major parts: the removable front wall cells; the vertical structure which connects the front wall cells to the headers; and the helium gas headers. The insert in Fig. 3 shows a cross section of the cell wall. As can be seen, it consists of a 0.9 cm thick backing capable of carrying the pressure stresses in the cylindrical cells and a thinner, 0.15 cm section enclosing small semi-circular tubes 1 cm in diameter running perpendicular to the cells. The thermal stress associated with the heat load on the front wall appears across the thin section only and is therefore minimized. This scheme has allowed the front wall to be designed to a maximum stress of 8500 psi.

The vertical structure, which is 48 cm high, anchors the front wall cells to the headers and also contains the conduits for the helium gas going to the front wall. This structure is welded to the bottom header plate and, together with the headers, constitutes the stiff support needed to sustain the vacuum load on the blanket wall.

There is concern about front wall failure or leaks which would require reactor shutdown. Two alternative schemes have been investigated to provide some redundancy on vacuum retainment. The first is to have two front walls with independent cooling and the second is to have a double layer of stainless steel as a containment skin on the semi-circular front wall cooling tubes. Both these approaches are being pursued further.

V. Summary

A detailed account of the conceptual tokamak reactor design study, UWMAK-II, has been presented and the key design features and technical problems have been discussed. Greater detail on many aspects of this study, as well as a description of the power cycle for UWMAK-II, will be presented in a future publication.^[27]

Acknowledgement: Research supported by the U.S.A.E.C. and the Wisconsin Electric Utility Research Foundation.

References

1. B. Badger et.al., "UWMAK-I, A Wisconsin Toroidal Fusion Reactor Design," UWFD-68, Nucl. Eng. Dept., Univ. of Wisc., Nov., 1973.
2. G. L. Kulcinski and R. W. Conn, Proc. 1st Nat'l Top. Conf. on Cont. Nucl. Fusion (CONF-740402-P1, U.S.A.E.C., April 1974) Vol. 1, p. 38.
3. R. W. Conn and G. L. Kulcinski, *ibid.*, Vol. 1, p. 56.
4. G. L. Kulcinski, R. W. Conn, G. Lang, "Carbon Curtain as a Low Z Liner for First Wall Protection and Impurity Control in Tokamaks," *Bull. Am. Phys. Soc.*, Oct., 1974 (to be published). See also UWFD-108, Univ. of Wisconsin Report, Aug., 1974.
5. G. L. Kulcinski, R. Brown, R. G. Lott, P. A. Sanger, *Nucl. Tech.* 22, (1974) 20.
6. D. Grove, private communication.
7. D. Meade, private communication.
8. H. A. Peterson, N. Mohan, W. C. Young, R. W. Boom, "Superconductive Inductor Converter Units for Pulsed Power Loads," Int'l. Conf. on Energy Storage, Compression, and Switching (Turin, Nov., 1974).
9. R. W. Boom, private comm. based on joint Univ. of Wisconsin - Fermi Accel. Lab. design to provide 10 sec power directly from the a.c. line.

10. D. G. McAlees and R. W. Conn, Nucl. Fus. 14, (1974) 419.
11. L. Artsimovich, JEPT Lett. 13, (1971) 70.
12. S. Yoshikawa, Phys. Rev. Lett. 25, (1970) 353.
13. A. A. Galeev and R. Z. Sagdeev, Sov. Phys.-JEPT, 53, (1967) 348.
14. B. B. Kadomtsev and O. P. Pogutse, Nucl. Fus. 11, (1971) 67.
15. S. O. Dean et.al., "Status and Objectives of Tokamak Systems for Fusion Research" (WASH-1295, U.S.A.E.C., 1974).
16. B. B. Kadomtsev and O. P. Pogutse, Sov. Phys. - Doklady 14, (1969) 470.
17. B. B. Kadomtsev and O. P. Pogutse, Sov. Phys. - JEPT 24, (1967) 1172.
18. A. A. Galeev, in Proc. 3rd Int'l Symp. on Tor. Plasma Conf. (Garching, 1973) paper E1-I.
19. Yu. I. Galushkim, V. I. Gervids and V. I. Kogan, Plasma Phys. and Cont. Nucl. Fus. (IAEA 1972) Vol. II, p. 407. See also, G.R. Hopkins, in Proc. Conf. on Cont. Th. Fus. Expts. (Conf-72111, USAEC, 1974) p. 795.
20. C. W. Horton, Jr., J. D. Callen, M. N. Rosenbluth, Phys. Fluids 14 (1971) 2019; see also D. E. Baldwin et.al., Plasma Phys. and Cont. Nucl. Fus. Research. (IAEA, 1972) Vol II, p. 735.
21. D. Düchs, G. Haas, D. Pfirsch, and H. Vernickel, J. Nucl. Mat. (to be published).
22. S. L. Gralnick, Nucl. Fus. 13 (1973) 703.
23. J. Purcell, H. Desportes, D. Jones, "Superconducting Magnet for the 15 foot NAL Bubble Chamber," (ANL-HEP-7215, Argonne National Lab., 1970).
24. J. Powell, F. T. Miles, A. Aronson, and W. F. Winsche, BNL-18236, Brookhaven National Laboratory (June 1973).
25. M. A. Abdou and C. W. Maynard, Proc. 1st Nat'l. Top. Conf. on Cont. Nucl. Fus. (CONF-740402-P1, U.S.A.E.C., April 1974) Vol. 1, p.685.
26. W. F. Vogelsang, G. L. Kulcinski, R. G. Lott, T. Sung, Nucl. Tech. 22(1974)379.
27. B. Badger et al., "UWMAK-II, A Helium Cooled, Stainless Steel, Conceptual Tokamak Power Reactor Design," UWFD-112, Nucl. Eng. Dept., Univ. of Wisconsin (to be published).